

# The influence of carbon dioxide on brain activity and metabolism in conscious humans

Feng Xu<sup>1,4</sup>, Jinsoo Uh<sup>1,4</sup>, Matthew R Brier<sup>2</sup>, John Hart Jr<sup>2</sup>, Uma S Yezhuvath<sup>1</sup>, Hong Gu<sup>3</sup>, Yihong Yang<sup>3</sup> and Hanzhang Lu<sup>1</sup>

<sup>1</sup>Advanced Imaging Research Center, University of Texas Southwestern Medical Center, Dallas, Texas, USA;

<sup>2</sup>Center for BrainHealth, University of Texas at Dallas, Dallas, Texas, USA; <sup>3</sup>Neuroimaging Research Branch, National Institute on Drug Abuse, National Institutes of Health, Baltimore, Maryland, USA

**A better understanding of carbon dioxide (CO<sub>2</sub>) effect on brain activity may have a profound impact on clinical studies using CO<sub>2</sub> manipulation to assess cerebrovascular reserve and on the use of hypercapnia as a means to calibrate functional magnetic resonance imaging (fMRI) signal. This study investigates how an increase in blood CO<sub>2</sub>, via inhalation of 5% CO<sub>2</sub>, may alter brain activity in humans. Dynamic measurement of brain metabolism revealed that mild hypercapnia resulted in a suppression of cerebral metabolic rate of oxygen (CMRO<sub>2</sub>) by 13.4% ± 2.3% (N = 14) and, furthermore, the CMRO<sub>2</sub> change was proportional to the subject's end-tidal CO<sub>2</sub> (Et-CO<sub>2</sub>) change. When using functional connectivity MRI (fcMRI) to assess the changes in resting-state neural activity, it was found that hypercapnia resulted in a reduction in all fcMRI indices assessed including cluster volume, cross-correlation coefficient, and amplitude of the fcMRI signal in the default-mode network (DMN). The extent of the reduction was more pronounced than similar indices obtained in **visual-evoked fMRI**, suggesting a **selective suppression effect** on resting-state neural activity. Scalp electroencephalogram (EEG) studies comparing hypercapnia with normocapnia conditions showed a **relative increase in low frequency power in the EEG spectra**, suggesting that the brain is entering a **low arousal state** on CO<sub>2</sub> inhalation.**

*Journal of Cerebral Blood Flow & Metabolism* (2011) 31, 58–67; doi:10.1038/jcbfm.2010.153; published online 15 September 2010

**Keywords:** carbon dioxide; cerebral metabolic rate of oxygen; electroencephalogram; functional connectivity MRI; hypercapnia

## Introduction

Carbon dioxide (CO<sub>2</sub>) is a potent vasodilator, and an increase of CO<sub>2</sub> in the inspired air is known to cause a number of vascular changes in the brain (Kastrup *et al*, 1999; Rostrup *et al*, 2000; Sicard and Duong, 2005), including increased cerebral blood flow (CBF), cerebral blood volume, as well as higher CO<sub>2</sub> and O<sub>2</sub> concentrations in the blood. The potential effect of CO<sub>2</sub> inhalation on neural activity is not clear. Existing literature mostly presumes that altering CO<sub>2</sub> partial pressure has no effect on brain tissue and the use of CO<sub>2</sub> inhalation or the carbonic anhydrase inhibitor acetazolamide can be considered

a purely vascular challenge to assess cerebrovascular reserve (de Boorder *et al*, 2004) or to calibrate functional magnetic resonance imaging (fMRI) signal (Chiarelli *et al*, 2007; Davis *et al*, 1998; Kim and Ugurbil, 1997).

Despite the wide acceptance and application of these assumptions in cerebrovascular research, some evidence suggested that the influence of CO<sub>2</sub> on brain activity merits more research. An important marker for tissue function, cerebral metabolic rate of oxygen (CMRO<sub>2</sub>), has been investigated under hypercapnia conditions. The results, however, were not consistent in the literature. A few studies (Barzilay *et al*, 1985; Kety and Schmidt, 1948; Novack *et al*, 1953) reported that CMRO<sub>2</sub> remains constant with hypercapnia, whereas other studies found a decrease (Kliefarth *et al*, 1979; Kogure *et al*, 1975; Sicard and Duong, 2005) or increase (Horvath *et al*, 1994; Jones *et al*, 2005; Yang and Krasney, 1995) in CMRO<sub>2</sub>. More recent findings in brain slices and anesthetized animals provided evidence at the cellular level that higher CO<sub>2</sub> partial pressure can have a profound effect on neural tissue including reducing pH, elevating adenosine concentration, and

Correspondence: Dr H Lu, Advanced Imaging Research Center, University of Texas Southwestern Medical Center, 5323 Harry Hines Boulevard, Dallas, TX 75390, USA.  
E-mail: hanzhang.lu@utsouthwestern.edu

<sup>4</sup>These authors contributed equally to this work.

This work was supported, in part, by the National Institutes of Health (Grants R01 MH084021, R01 NS067015, R01 AG033106, and R21 EB007821).

Received 2 April 2010; revised 2 July 2010; accepted 4 August 2010; published online 15 September 2010

suppressing synaptic potentials (Dulla *et al*, 2005; Gourine *et al*, 2005; Zappe *et al*, 2008b). However, these previous studies were largely performed under laboratory conditions, and it is unclear if the results were influenced by certain factors including the anesthetic agent, which by itself will reduce neural activity (Shulman *et al*, 1999). We are therefore interested in conducting measurements in conscious human subjects under physiologically relevant conditions.

The study of neural response to CO<sub>2</sub> pressure change is particularly challenging compared with studies using sensory, motor, or cognitive stimuli. Traditional tools such as PET, fMRI, and optimal imaging are not readily usable, because these methods all use vascular response as a surrogate for neural function (Fox and Raichle, 1986). However, CO<sub>2</sub> is known to have a strong vascular effect that is present even if neural activity does not change (e.g., it has been shown to change vessel size even in dissected blood vessels). Therefore, an observation of altered blood flow, blood volume, or BOLD fMRI signal alone would not necessarily suggest a change in neural activity (Biswal *et al*, 1997). In fact, the vascular effect of CO<sub>2</sub> may be a nuisance in the study of tissue. It is perhaps for these reasons that the exact influence of CO<sub>2</sub> inspiration on neural activity is not fully characterized to date (Horvath *et al*, 1994; Jones *et al*, 2005; Kety and Schmidt, 1948; Kliefoth *et al*, 1979).

This study used three noninvasive techniques to assess the effect of breathing a CO<sub>2</sub>-enriched air (5% CO<sub>2</sub>, 21% O<sub>2</sub>, and 74% N<sub>2</sub>) on brain tissue. We have recently developed an MRI technique to quantify *CMRO*<sub>2</sub> (Lu and Ge, 2008; Xu *et al*, 2009), allowing us to assess the effect of CO<sub>2</sub> on neural metabolism. In the first study, we compared the participant's *CMRO*<sub>2</sub> levels when breathing CO<sub>2</sub>-enriched gases (referred to as hypercapnia) to breathing normal room-air gases (normocapnia). In the second study, we investigated the spontaneous neural activity under normocapnia and hypercapnia conditions by performing functional connectivity MRI (fcMRI). Finally, neural electrical potential was investigated directly by scalp electroencephalogram (EEG) under room-air and CO<sub>2</sub> breathing conditions.

## Materials and methods

### Participants

A total of 50 healthy subjects (27.9 ± 6.5 years old, 32 males and 18 females) were studied. Each subject gave an informed written consent before participating in the study. The study protocol was approved by the Institutional Review Board of the University of Texas Southwestern Medical Center. These subjects were divided into four groups for different arms of the study. Fourteen subjects were studied to assess the effect of CO<sub>2</sub> inhalation on *CMRO*<sub>2</sub>. Ten subjects were studied in the *CMRO*<sub>2</sub> sham control study. Fourteen subjects were studied to assess the

effect of CO<sub>2</sub> on resting-state functional connectivity. Twelve subjects were studied to assess the effect of CO<sub>2</sub> on EEG spectra.

### Carbon Dioxide Manipulation

Carbon dioxide delivery was achieved by using a gas delivery system created in our laboratory, with only nonmetallic components (see Supplementary Figure S1 for a diagram). With this system, a change in gas content can be made without stopping the scan or recording and without moving the subject. Other details of the CO<sub>2</sub> manipulation are described in Supplementary Text.

### Measurement of Global Cerebral Metabolic Rate of Oxygen

Measurement of *CMRO*<sub>2</sub> was performed on a 3 Tesla MRI system (Philips Medical Systems, Best, The Netherlands) using a noninvasive technique (Lu and Ge, 2008; Xu *et al*, 2009). Briefly, *CMRO*<sub>2</sub> in units of μmol/min was calculated using Fick principle:

$$CMRO_2 = CBF(Y_a - Y_v)C_a \quad (1)$$

where *CBF* is the blood flow in mL/min, *Y<sub>a</sub>* is the arterial oxygenation, *Y<sub>v</sub>* is the venous oxygenation, *C<sub>a</sub>* is the amount of oxygen molecules that a unit volume of blood can carry, assumed to be 833.7 μmol O<sub>2</sub>/100 mL blood based on physiology literature (Guyton and Hall, 2005). The *CBF* was measured with phase-contrast MRI, *Y<sub>a</sub>* was determined by a pulse oximeter; *Y<sub>v</sub>* was estimated with a recently developed technique, T2-relaxation-under-spin-tagging MRI (Lu and Ge, 2008). The details of the imaging parameters are described in Supplementary Text.

The experiment began with the subject breathing room-air for 4 minutes, establishing a normocapnic state, during which *CMRO*<sub>2</sub> was determined. The subject was then switched to the gas mixture containing 5% CO<sub>2</sub> and continued to breath for another 6 minutes. We waited for 2 minutes to allow for physiological stabilization in the hypercapnic state (Figure 1). The *CMRO*<sub>2</sub> was measured again in the last 4 minutes under stable hypercapnia condition.

The data processing procedures for T2-relaxation-under-spin-tagging MRI and phase-contrast MRI were based on an algorithm described previously (Lu and Ge, 2008; Xu *et al*, 2009) and are described in Supplementary Text and Supplementary Figure S2. The arterial blood oxygenation, *Y<sub>a</sub>*, was recorded at 1 sample/s and the data corresponding to MRI acquisition period (about 4 minutes) were averaged to yield the final value.

Once *Y<sub>a</sub>*, *Y<sub>v</sub>*, and *CBF* were obtained, *CMRO*<sub>2</sub> was calculated from these variables using equation (1). The *CMRO*<sub>2</sub> values during normocapnia and hypercapnia were compared using a paired Student's *t*-test. A *P* value of <0.05 was considered statistically significant.

A sham control study was conducted in a group of healthy subjects (*N*=10, age 28.7 ± 5.7 years, 6 males, 4 females), in which the subject was given the same instruction as the real CO<sub>2</sub> study (they were told that they

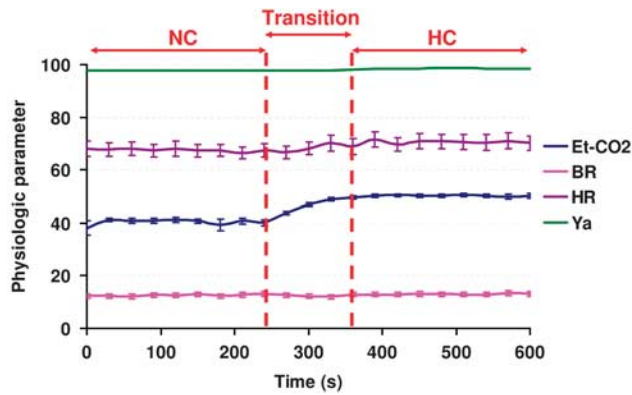


**Figure 1** Time courses of physiologic parameters under normocapnia (NC) and hypercapnia (HC) conditions. End-tidal (Et) CO<sub>2</sub>, heart rate (HR), breathing rate (BR), and arterial oxygenation (Y<sub>a</sub>) were monitored and recorded during the cerebral metabolic rate of oxygen (CMRO<sub>2</sub>) experiments. After the gas valve was switched to the CO<sub>2</sub> mixture, the first 2 minutes were considered as a transition period, during which no magnetic resonance imaging (MRI) measurements were made. Error bars indicate standard errors of mean across subjects ( $N = 14$ ). Hypercapnia resulted in an increase in Et-CO<sub>2</sub>, HR, and Y<sub>a</sub> ( $P < 0.05$ ). The BR did not show a significant change.

will inhale CO<sub>2</sub>), but the gas valve was on room-air for the entire duration of the experiment. This was conducted to rule out the possibility that the observed CMRO<sub>2</sub> change in the CO<sub>2</sub> breathing task was due to mental stress or the subject becoming anxious, drowsy, and/or sleepy after being inside the magnet. All other procedures and MRI scans were identical to the real CO<sub>2</sub> study.

### Functional Connectivity Magnetic Resonance Imaging

The fMRI scans were performed while the subjects were fixated on a crosshair. For comparison, a visual-task fMRI using a flashing checkerboard was also performed. The details of the imaging parameters are described in Supplementary Text. Each scan was performed twice, first under a normocapnia condition and the other under a hypercapnia condition. Similar to the CMRO<sub>2</sub> studies, we waited for 2 minutes to allow a transition between normocapnic and hypercapnic conditions.

We used AFNI (NIMH Scientific and Statistical Computing Core, Bethesda, MD, USA) and in-house Matlab scripts for fMRI and visual fMRI data processing. The processing of visual fMRI used standard procedures and is described in Supplementary Text. The steps of the fMRI processing followed those described by Hong *et al* (2009). Briefly, each data set was preprocessed with slice timing correction, motion correction (realignment), removal of the linear trend, transformation to standard Talairach space (matrix =  $61 \times 73 \times 61$ , resolution =  $3 \times 3 \times 3$  mm<sup>3</sup>), and smoothing by a Gaussian filter with a full width at half maximum of 6 mm. The fMRI data were then analyzed using a seed-based approach to identify the resting-state networks. Low-pass filtering (cutoff frequency = 0.1 Hz) was applied to the preprocessed signal time course on a voxel-by-voxel basis. Cardiac and respiratory pulsation effects were removed

using the respiratory belt and pulse sensor that are integrated into the MRI system. The fluctuations of end-tidal CO<sub>2</sub> (Et-CO<sub>2</sub>) and the whole brain averaged fMRI signal were also removed from the subject's voxel time course. For the default-mode network (DMN), seed regions of interest (ROIs) (size = 0.73 cm<sup>3</sup>) were positioned at bilateral posterior cingulate cortices based on Talairach coordinates. The cross-correlation coefficient (cc) between these seed voxels and all other voxels was calculated to generate a correlation map. Then, a Fisher-z transform was used and a group analysis was performed on the z-maps of all subjects to identify the DMN (threshold:  $P < 0.005$ , cluster size > 2.7 cm<sup>3</sup>). The data sets from normocapnia and hypercapnia conditions were analyzed separately.

Three fMRI indices were compared between the normocapnia and hypercapnia conditions. An index of volume of correlated clusters was defined as the total number of voxels that are significantly correlated with the seed ROI (excluding the voxels in the seed cluster). The cc between the seed voxels and the voxels delineated in the correlated clusters was calculated. To avoid the confounding effect of volume differences between normocapnia and hypercapnia, only the voxels that were detected in both conditions (i.e., overlapping voxels) were included in the cc analysis. As a third index, the amplitude of fMRI signal fluctuation was calculated. As there is not a ubiquitously defined parameter for fMRI amplitude, we used an index that is equivalent to the percentage signal change in conventional fMRI. The fMRI signal,  $S_{\text{fMRI}}$ , is defined as follows. Let  $x$  and  $y$  be the time courses of seed voxels and the voxels in the correlated clusters in fMRI. Then,  $S_{\text{fMRI}}$  is calculated by a linear regression on:  $y' = S_{\text{fMRI}} x'$ , where  $x' = (x - \text{mean}(x)) / (2 \|x - \text{mean}(x)\| / \sqrt{n_{\text{dyn}}})$  and  $y' = (y - \text{mean}(y)) / \text{mean}(y)$ . In this expression, 'mean' indicates the mean signal intensity of the time course,  $n_{\text{dyn}}$  is the number of points in the time course, and the operator  $\| \bullet \|$  indicates 2-norm. A desirable feature of this index is that, if we apply this calculation to a conventional fMRI data set with the voxel time course as  $y$  and the fMRI paradigm as  $x$ , the resulting value would be exactly the same as BOLD percentage change obtained from a typical fMRI general linear model analysis. Using this index, the CO<sub>2</sub> effect on fMRI signal can be feasibly compared with that on visual-evoked fMRI signal.

It should be noted that these hypercapnia-induced decreases in fMRI signal may be caused by a combined effect of CO<sub>2</sub> on electrophysiological signal and on basal vascular state (Cohen *et al*, 2002), which has a modulatory effect on BOLD signal amplitude. Therefore, we defined a normalized fMRI signal amplitude (calculated for each individual),  $S_{\text{fMRI},n} = S_{\text{fMRI}} / S_{\text{fMRI}}$ , where a visual-evoked fMRI,  $S_{\text{fMRI}}$ , is used as a reference to eliminate the vascular effect from fMRI signal. This calculation assumed that differences in  $S_{\text{fMRI}}$  between normocapnia and hypercapnia were primarily due to vascular effect of CO<sub>2</sub>. Previous studies have shown that visual-evoked EEG response is minimally affected by the CO<sub>2</sub> level (Jones *et al*, 2005; Zappe *et al*, 2008b). With the assumption that EEG response provides a reasonable indication of electrophysiological response, we hypothesize that visual-evoked electrophysiological response is also independent of CO<sub>2</sub>



level. Thus, the visual fMRI signal difference comparing normocapnia and hypercapnia is solely due to the vascular effect. A more detailed description and justification of the normalization calculation is described in Supplementary Text.

In addition to the DMN, sensorimotor regions were also identified from the fcMRI data. The seed regions were positioned in the right motor cortex and the voxels correlating with the seed time course were identified. We have also tested using the left motor cortex for seed regions and the results were similar. Comparison was made between normocapnia and hypercapnia conditions.

## Electroencephalogram

We used a 64-channel SynAmps II EEG system (Neuro Scan, Charlotte, NC, USA), which included an EEG cap on which the geometric locations of the electrodes are preset. Saline was applied in each electrode to ensure proper electrode conduction, the impedance of which is monitored on a computer screen. To avoid mechanical pressure on the electrodes, these experiments were conducted with subject sitting upright, unlike the MRI experiments in which the subjects were at supine position. We assumed that the CO<sub>2</sub> effect, if any, is comparable between these two body positions. The subjects were instructed to keep their eyes open and fixate on a white cross throughout the experiments. This control of eye fixation is important as it can change the EEG power spectra (Kiloh *et al*, 1972).

The experiments were conducted for 17 minutes during which time the subjects were breathing room-air for 5 minutes, switched to the 5% CO<sub>2</sub> gas mixture for 7 minutes and then returned to room-air for the final 5 minutes. The EEG recordings were made continuously during this 17-minute period. The EEG data from the first and second normocapnia periods were combined to yield an interpolated signal that will be compared with the signal of the hypercapnia period. The interpolation computation was necessary to correct for linear trends, hysteresis, and rebound effects in the recordings (Zappe *et al*, 2008b), which could cause a signal drift over time.

The data were recorded with a reference electrode located near the vertex, resulting in small amplitudes over the top of the head. To eliminate this effect, the data were rereferenced to the average potential over the entire head, which approximates the voltages relative to infinity. To reduce a slight bias in the electrode-based average reference, spherical splines were fit to the data and used to compute the average. Other details of the EEG processing procedures are described in Supplementary Text.

Power spectra of three frequency bands were investigated based on well-established frequency definition: 1 to 3 Hz for  $\delta$  band, 4 to 7 Hz for  $\theta$  band, and 8 to 13 Hz for  $\alpha$  band (Kiloh *et al*, 1972). The analysis was performed for each of the channels as well as for the average of all channels.

## Results

Inhalation of 5% CO<sub>2</sub> increased the subjects' Et-CO<sub>2</sub> from  $41.3 \pm 0.8$  mm Hg ( $N=14$ , 9 males and 5 females,

mean  $\pm$  s.e.m.) to  $50.1 \pm 0.7$  mm Hg ( $P<0.001$ ). Figure 2A shows representative T2-relaxation-under-spin-tagging MRI data for the normocapnia and hypercapnia conditions. The MR T<sub>2</sub> signal decay is much slower during hypercapnia, suggesting a longer venous blood T<sub>2</sub>. Accordingly, venous oxygenation,  $Y_v$ , was found to increase significantly (paired  $t$ -test,  $P<0.001$ ) from normocapnia to hypercapnia (Table 1). Arterial oxygenation ( $Y_a$ ) measured by pulse oximeter showed a negligible change between the two conditions (Table 1). Thus, the oxygen extraction fraction, i.e.,  $Y_a - Y_v$ , reduced considerably (Table 1). Figure 2B shows representative phase-contrast MRI results. One can see a clear increase of flow velocity as indicated by darker pixel intensity (arrows). Quantitative analysis revealed that CBF increased significantly from normocapnia to hypercapnia ( $P<0.001$ ). Table 1 summarizes the values of the physiologic parameters during normocapnia and hypercapnia conditions. The relative changes are plotted in Figure 2C. Using equation (1),  $CMRO_2$  was estimated and found to show a reduction of  $13.4\% \pm 2.3\%$  comparing hypercapnia with normocapnia ( $P<0.001$ ). That is, in addition to the pronounced vascular effect, high CO<sub>2</sub> content also modestly reduces tissue's metabolic rate. In the sham study,  $CMRO_2$  values during the baseline and sham control periods were  $977.6 \pm 88.5$   $\mu$ mol/min and  $995.4 \pm 89.4$   $\mu$ mol/min, respectively, and did not show a difference ( $P=0.34$ , paired  $t$ -test,  $N=10$ ) (see Supplementary Table S1).

We further hypothesized that CO<sub>2</sub> has a dose-dependent effect on  $CMRO_2$  where an individual with a smaller Et-CO<sub>2</sub> change during the hypercapnic phase will have a smaller change in  $CMRO_2$  and vice versa. Figure 3 shows a scatter plot between Et-CO<sub>2</sub> change and  $CMRO_2$  change across the 14 subjects studied. A significant correlation ( $P=0.014$ ) was observed.

Figure 4 shows DMN in both the normocapnia and hypercapnia conditions identified from the fcMRI data ( $N=14$ ). The DMN under normocapnia condition (Figure 4A) clearly illustrates the connectivity among posterior cingulate cortex (seed region), bilateral inferior parietal regions, medial prefrontal cortex, and medial temporal lobe. In contrast, cluster volume under hypercapnia condition (Figure 4B) shows a drastic reduction. Similarly, the cc values between the seed region and the other DMN regions were reduced significantly (paired  $t$ -test  $P=0.024$ ) comparing hypercapnia with normocapnia. The amplitude of fcMRI signal also showed a reduction by 37.2% due to hypercapnia ( $P=0.001$ ). The application of similar analysis to the visual fMRI data revealed that the activation volume, cc, and fMRI signal amplitude were reduced by 13.5%, 2.4%, and 22.1%, respectively, when comparing results under hypercapnia with that under normocapnia (Table 2). All indices showed smaller hypercapnia-induced changes compared with those in the fcMRI data. The normalized fcMRI signals were

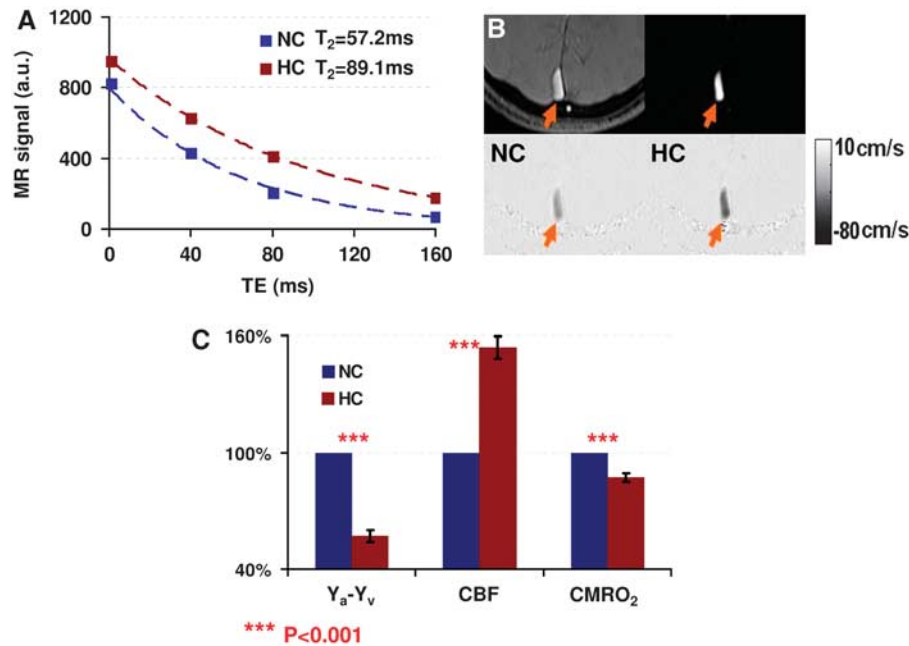


**Figure 2** Magnetic resonance imaging (MRI) measurement of cerebral metabolic rate of oxygen (CMRO<sub>2</sub>) under normocapnia (NC) and hypercapnia (HC) conditions. **(A)** Venous oxygenation, Y<sub>v</sub>, used in the CMRO<sub>2</sub> calculation was measured with a T<sub>2</sub>-relaxation-under-spin-tagging (TRUST) MRI technique. The MR signal in the venous blood was measured as a function of TE. The decay time constant is the blood T<sub>2</sub>, which can be converted to blood oxygenation. The time constant during hypercapnia (HC, red) is longer than that in normocapnia (NC, blue). **(B)** Cerebral blood flow (CBF) used in the CMRO<sub>2</sub> calculation was measured with phase-contrast MRI applied in the sagittal sinus. The four images are: raw image, magnitude image, velocity map during NC, and velocity map during HC. Arrows indicate the sagittal sinus. In the velocity maps, the darker color indicates higher outflow velocity. **(C)** Summary of CO<sub>2</sub>-induced changes in Y<sub>a</sub>-Y<sub>v</sub>, CBF, and CMRO<sub>2</sub> (N = 14). The parameter values under normocapnia were set as 100%. The values under hypercapnia condition were presented relative to the normocapnia values.

**Table 1** Summary of vascular and metabolic parameters under normocapnia and hypercapnia conditions

	Y <sub>v</sub>	Y <sub>a</sub>	Y <sub>a</sub> -Y <sub>v</sub>	CBF (mL/min)	CMRO <sub>2</sub> (μmol/min)
Normocapnia	0.624 ± 0.017	0.979 ± 0.003	0.355 ± 0.067	352.8 ± 16.8	1042.3 ± 76.1
Hypercapnia	0.782 ± 0.014	0.985 ± 0.002	0.203 ± 0.055	547.1 ± 35.6	899.0 ± 66.1
Relative change	26.1%	0.6%	-42.6%	54.5%	-13.4%
P value (paired t-test)	<0.001	<0.001	<0.001	<0.001	<0.001

CBF, cerebral blood flow; CMRO<sub>2</sub>, cerebral metabolic rate of oxygen.

0.29 ± 0.03 and 0.23 ± 0.02 for normocapnia and hypercapnia, respectively, showing a 20.1% reduction (P=0.020). In addition to the DMN brain regions, we have studied the sensorimotor regions, which also have a well-defined resting-state network (Biswal *et al*, 1995; Xiong *et al*, 1999). Reductions similar to that observed for the DMN were observed comparing hypercapnia with normocapnia (see Supplementary Figure S3 and Supplementary Table S2 for details).

The EEG recordings with scalp electrodes were compared between normocapnia and hypercapnia conditions (N=12). Table 3 shows the EEG signal power in δ band (1 to 3 Hz), θ band (4 to 7 Hz), and α band (8 to 13 Hz) under normocapnia and hypercapnia conditions. The signal power was significantly

increased in the δ band (P=0.049), accompanied by a significant decrease in the α band (P=0.003) (Figure 5). The θ band power did not show a significant change. Therefore, the relative EEG power was shifted toward the lower frequency range, a typical pattern of reduced brain arousal state (Kiloh *et al*, 1972). Figure 6 shows the topographic maps of EEG power in different frequency bands during normocapnia and hypercapnia conditions, as well as the power ratio. The data suggest that the slowing of the EEG signal appeared to be present in all electrodes across the entire brain. We have also studied frequency ranges beyond 13 Hz (e.g., β band, γ band), but the signal was small and statistical comparisons did not yield significant differences between the two conditions.

## Discussion

This study investigated the effect of blood CO<sub>2</sub> levels on brain activity from a number of perspectives. We first showed that hypercapnia reduced metabolic activity in the brain. Second, neural activity was

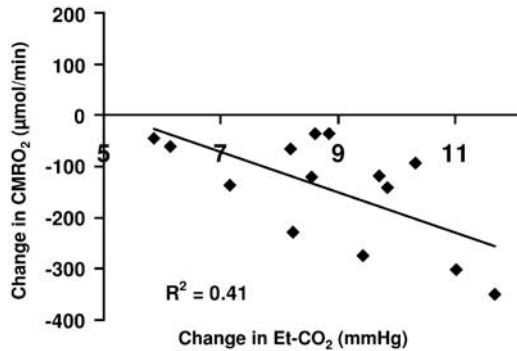


**Figure 3** Scatter plot between hypercapnia-induced end-tidal CO<sub>2</sub> (Et-CO<sub>2</sub>) change and cerebral metabolic rate of oxygen (CMRO<sub>2</sub>) change across subjects ( $N = 14$ ). Inhalation of 5% CO<sub>2</sub> caused an increase in Et-CO<sub>2</sub> and a decrease in CMRO<sub>2</sub> in all subjects studied. Different subjects have slightly different Et-CO<sub>2</sub> change. Individuals with a greater Et-CO<sub>2</sub> change tended to have a greater CMRO<sub>2</sub> change ( $P = 0.014$ ), suggesting a dose-dependent effect of CO<sub>2</sub> on brain metabolism.

assessed indirectly by BOLD fMRI and the data suggested that CO<sub>2</sub> inhalation caused a decrease in spontaneous brain connectivity. Finally, EEG was used as a direct measure of neural activity and the results showed that hypercapnia caused a relative increase in lower frequency power spectra. Overall, our data showed a suppressive effect of CO<sub>2</sub> on brain activity.

The findings from this study are in general agreement with earlier studies conducted in animals. In a study of macaque monkeys under anesthesia, Zappe *et al* (2008b) reported that hypercapnia induced a 15% reduction in resting-state multiunit neural activity in the primary visual cortex. Although the authors did not investigate other brain regions in the study (personal communications), previous literature suggests that this depression effect is likely to be global (Kliefth *et al*, 1979). Our study represents the first systematic investigation of this effect in conscious humans and suggests that resting-state neural activity is reduced due to mild hypercapnia. Further, we showed that this suppression of neural activity is accompanied by a reduction in metabolic activity of similar amplitude.

A number of studies in the literature have compared CMRO<sub>2</sub> between normocapnia and hypercapnia conditions. Our finding of a 13% decrease is

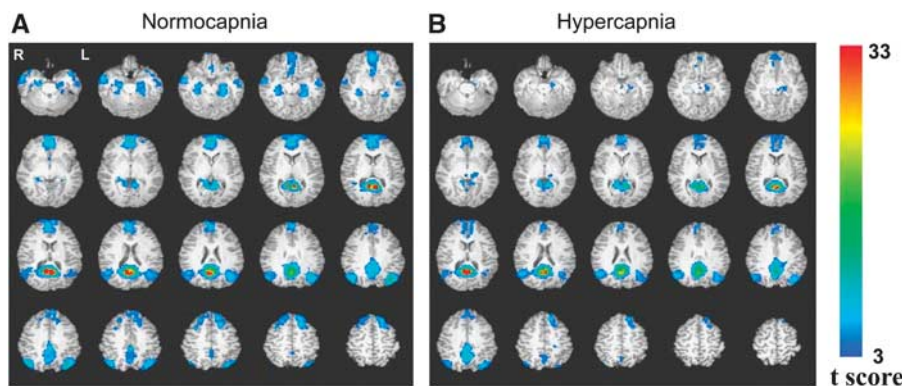


**Figure 4** Resting-state default-mode network (DMN) under normocapnia (A) and hypercapnia (B) conditions ( $N = 14$ ). The DMN regions consist of posterior cingulate cortex, bilateral inferior parietal cortex, medial frontal cortex, and bilateral medial temporal lobe, as defined by many previous studies. Hypercapnia resulted in a significant reduction in the size of the cluster volume.

**Table 2** Summary of resting-state default-mode network parameters during normocapnia and hypercapnia

	Et-CO <sub>2</sub> (mmHg)	Cluster volume (mL)		Correlation coefficient		Signal amplitude (%)		
		DMN fMRI	Visual fMRI	DMN fMRI	Visual fMRI	DMN fMRI	Visual fMRI	Normalized fMRI
Normocapnia	40.2 ± 0.7	120.4	206.9	0.67 ± 0.03	0.69 ± 0.04	0.29 ± 0.02	1.02 ± 0.07	0.29 ± 0.03
Hypercapnia	47.4 ± 0.7	54.3	178.9	0.55 ± 0.05	0.68 ± 0.03	0.18 ± 0.02	0.80 ± 0.08	0.23 ± 0.02
Relative change	18.0%	-54.9%	-13.5%	-17.6%	-2.4%	-37.2%	-22.1%	-20.1%
<i>P</i> value (paired <i>t</i> -test)	<0.001	N/A <sup>a</sup>	N/A <sup>a</sup>	0.024	0.30	0.001	0.018	0.020

DMN, default-mode network; Et-CO<sub>2</sub>, end-tidal carbon dioxide; fMRI, functional connectivity magnetic resonance imaging.

For comparison, visual-evoked fMRI results are also shown.

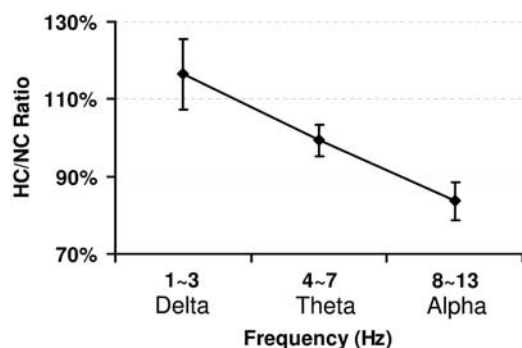
<sup>a</sup>This index was obtained from a group analysis, thus the value does not have a s.d. or an associated *P* value.



**Table 3** EEG power in different frequency bands under normocapnia and hypercapnia conditions

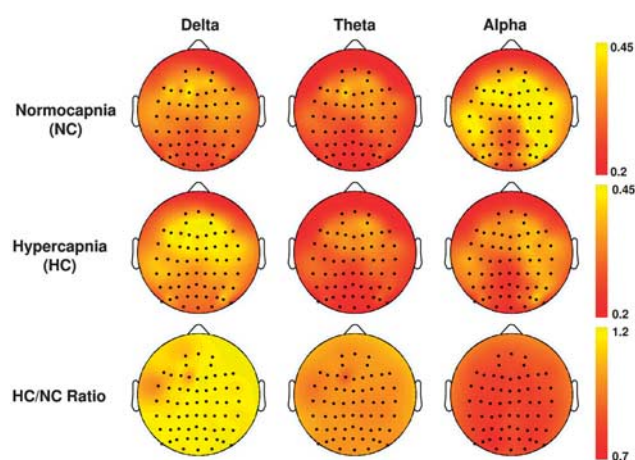
Frequency band	$\delta$	$\theta$	$\alpha$
Frequency range	1–3	4–7	8–13
Normocapnia power ( $\mu V^2$ )	$6.4 \pm 0.7$	$6.4 \pm 0.9$	$10.2 \pm 2.1$
Hypercapnia power ( $\mu V^2$ )	$7.6 \pm 1.1$	$6.3 \pm 1.0$	$8.1 \pm 1.8$
Ratio between hypercapnia power and normocapnia power	1.16	0.99	0.84
<i>P</i> value	0.049	0.440	0.003

EEG, electroencephalogram.

**Figure 5** Relative changes in electroencephalogram (EEG) signal power comparing hypercapnia with normocapnia. The powers under normocapnia condition were set as 100%. Hypercapnia resulted in a slowing of the EEG power spectra, with  $\delta$  band (1 to 3 Hz) showing a power increase and  $\alpha$  band (8 to 13 Hz) showing a decrease.

in general agreement with the reports by Kogure *et al* (1975) (–15%), Sicard and Duong (2005) (–10%), Barzilay *et al* (1985) (–15%), and Kliefloth *et al* (1979) (–30%), but is inconsistent with those reported by Kety and Schmidt (1948) (+3%), Novack *et al* (1953) (0%), Yang and Krasney (1995) (+17%), and Horvath *et al* (1994) (+35%). Possible reasons for the discrepancy include different measurement techniques, different species and the effect of anesthetic agent. Specifically, only the earlier studies by Kety and Schmidt (1948) and Novack *et al* (1953) used human subjects, and the more recent studies all used animal subjects under anesthesia. It is known that anesthetic agent itself may affect neural activity and metabolism (Shulman *et al*, 1999).

A change in  $CMRO_2$  because of hypercapnia also has important implications for calibrated fMRI. Calibrated fMRI is an approach to obtain quantitative changes in brain metabolism during neural activation (Chiarelli *et al*, 2007; Davis *et al*, 1998; Kim and Ugurbil, 1997). This technique often uses CO<sub>2</sub> inhalation to determine the calibration factor and assumes that mild hypercapnia does not alter  $CMRO_2$ . In the case that CO<sub>2</sub> does cause a decrease in  $CMRO_2$ , the theoretical framework of calibrated fMRI will remain valid but the processing of experimental data should be adjusted slightly. Specifically, the *M* factor in calibrated fMRI will

**Figure 6** Topographic maps of electroencephalogram (EEG) signals under normocapnia and hypercapnia conditions (*N* = 12). The EEG signal power was calculated for each frequency band. In the topographic maps, the nose of the subject is on the top, illustrated by the triangle. The ears are illustrated by the rectangles. Each black dot indicates one electrode. The bottom row shows the ratio between hypercapnia and normocapnia signals. It can be seen that the  $\delta$  power increased during hypercapnia, whereas the  $\alpha$  power decreased. The  $\theta$  power remained unchanged. From the ratio map, it can also be seen that hypercapnia-induced changes affected all electrodes. The maps shown were averages of all subjects studied. Before averaging, the EEG power of each subject was normalized to the electrode-averaged power under normocapnia, so that the variations in EEG signal power (e.g., because of differences in scalp thickness) between subjects are accounted for.

become lower, the estimated  $CMRO_2$  will be smaller, and the  $CBF/CMRO_2$  coupling factor *n* will be greater. Interestingly, these trends will shift the MRI results to become more comparable to earlier reports using PET (Fox and Raichle, 1986).

Our observation of a reduced functional connectivity during CO<sub>2</sub> breathing is consistent with previous reports that light sedation (Greicius *et al*, 2008) or anesthesia (Deshpande *et al*, 2010) decreases connectivity in DMN regions, and is also in line with the suggestions that CO<sub>2</sub> has a mild sedative effect (Fukuda *et al*, 2006). The CO<sub>2</sub>-induced reduction in sensorimotor connectivity is also in good agreement with a previous report by Biswal *et al* (1997). In our study, we have taken special precaution to minimize the influence of basal vascular state on BOLD signals, which were not accounted for in previous studies comparing fcMRI data across physiologic states (Biswal *et al*, 1997; Deshpande *et al*, 2010; Greicius *et al*, 2008; Horovitz *et al*, 2009). We have used visual-evoked fMRI signal as a reference with the assumption that the alterations in fMRI signal is solely due to a change in vascular state (Jones *et al*, 2005; Zappe *et al*, 2008a). Although this referencing strategy is still based on assumptions and biophysical models (Davis *et al*, 1998; Jones *et al*, 2005; Zappe *et al*, 2008a), it nonetheless provides an additional level of control

for nonneuronal effect and is the best available technique to our knowledge. Our results demonstrated that the 'normalized' fcMRI signal still showed a significant decrease because of hypercapnia, suggesting that some of the fcMRI signal reduction is of neuronal origin. We have also applied similar normalization procedures to the activation volumes and cc values, and the results showed that the normalized cc showed significant hypercapnia-related reduction ( $P=0.03$ ), although the cluster volume did not show significant changes.

In this study, we found a relative increase in low frequency EEG power spectra on inducing hypercapnia. It is known that EEG frequency is highly dependent on the physiologic state of an individual (Kiloh *et al*, 1972). If the brain is in a high arousal state (e.g., conversation, thinking), the EEG power spectra show a relative increase in higher frequencies, whereas if the brain is in a low arousal state (e.g., relaxing, drowsy, sleepy, day dreaming) lower frequencies predominate. Our data suggest that during hypercapnia, the brain's electrical activity resembles lower arousal states. This finding is consistent with reports that mild hypercapnia may improve the duration and efficiency of sleep (Fragne *et al*, 2008). This study has focused on the effect of CO<sub>2</sub> inhalation on resting-state EEG. Using intracortical recordings in anesthetized monkeys, Zappe *et al* (2008a) suggested that relative changes in visual-evoked EEG are not affected by CO<sub>2</sub> inhalation. Further work is needed to determine whether this finding is applicable for absolute EEG signal changes in awake humans.

The findings from the three complementary techniques are in general agreement with each other. Our observation that a lower metabolic state corresponds to a slower EEG signal is in agreement with reports by Maandag *et al* (2007) that neurons under low metabolic state have a slower oscillation frequency. The total EEG power in our data did not change from normocapnia to hypercapnia ( $P=0.36$ ). Although this observation seems to be contradictory to the reduced metabolic rate, a number of previous studies have shown that the relationship between metabolism and EEG signal is frequency dependent (Alper *et al*, 2006; Buchan *et al*, 1997). Buchan *et al* (1997) compared EEG and oxygen metabolism in Alzheimer's patients and found that EEG and metabolic rate were positively correlated in frequency components above 8 Hz but they were negatively correlated in frequencies lower than 6 Hz. These findings are consistent with our observations that decreased metabolic rate is accompanied by decreased  $\alpha$  band (8 to 13 Hz) power and increased  $\delta$  band (1 to 3 Hz) power. The relationship between fcMRI and EEG signals has also been studied by a number of investigators, and the majority of the reports appear to suggest that fcMRI signal has a correlation with  $\alpha$  power in the EEG (Mantini *et al*, 2007; Moosmann *et al*, 2003). Thus, our observation of a concomitant reduction in fcMRI signal and  $\alpha$  power during hypercapnia is in general

agreement with this notion. Another evidence of a link between fcMRI and EEG comes from studies using simultaneous EEG-fcMRI recordings during sleep (Horovitz *et al*, 2009). It has been shown that a slowing of EEG (i.e., greater  $\delta$  power) is accompanied by reduced functional connectivity among selective DMN regions (Horovitz *et al*, 2009). However, it is not straightforward to directly compare our findings of CO<sub>2</sub> effects to deep sleep, because the neural activity changes during sleep are likely more complex than those because of CO<sub>2</sub> inhalation.

The mechanism of the observed suppression of CMRO<sub>2</sub> is not clear. A few *in vitro* studies suggested that it may be related to tissue acidosis when carbonic acid is formed from CO<sub>2</sub> and water. In a study using brain slices, Dulla *et al* (2005) found that increased CO<sub>2</sub> pressure reduces pH in the extracellular space, which increases the extracellular adenosine concentration. Gourine *et al* (2005) suggested that ATP release may be involved in the CO<sub>2</sub> sensing pathways.

The reduction in spontaneous neural activity as shown by the fcMRI data is also consistent with reports that exposure to hypercapnia can terminate epileptic bursting. In laboratory settings, CO<sub>2</sub> breathing has also been shown to terminate some epileptic seizure activity (Dulla *et al*, 2005). In addition, acetazolamide, sold under the trade name 'Diamox', is a carbonic anhydrase inhibitor and increases CO<sub>2</sub> pressure in the blood. This drug is commonly used as a vasodilator in the assessment of vascular reserve and cerebrovascular function. Interestingly, acetazolamide is also an antiepileptic drug that is used to treat certain types of epilepsy (e.g., absence epilepsy, myoclonic seizure, catamenial epilepsy) (Levy *et al*, 1995). Intake of acetazolamide and inhalation of CO<sub>2</sub> have virtually the same effect and are often considered the same physiologic challenge in the cerebrovascular literature. Therefore, it is reasonable to expect that CO<sub>2</sub> inhalation may also have an antiepileptic effect. Another line of supporting evidence for the CO<sub>2</sub> effect is that hyperventilation causes hypocapnia, and has been known to induce interictal spike-and-wave activity (Niedermeyer and da Silva, 2005).

In the previously mentioned calculation of CMRO<sub>2</sub>, we have only considered oxygen bound to hemoglobin but did not account for oxygen that is dissolved in the plasma. This assumption is considered reasonable in our experiments because the majority (>98%) of the oxygen molecules carried by the blood is in the form of hemoglobin-bound oxygen. To confirm this point, we have incorporated an oxygen sensor in our gas apparatus and measured Et-O<sub>2</sub> pressure in four subjects outside the MRI room. This showed that Et-O<sub>2</sub> under normocapnia and hypercapnia conditions were  $114.7 \pm 3.1$  mm Hg and  $136.6 \pm 2.3$  mm Hg, respectively. The difference is presumably due to hyperventilation when the subject breathes CO<sub>2</sub>. By estimating the amount of dissolved oxygen from Et-O<sub>2</sub> (Guyton and Hall,



2005),  $CMRO_2$  during normocapnia and hypercapnia was recalculated and the results still showed a reduction of  $CMRO_2$  by  $10.4\% \pm 2.2\%$ .

The normalization calculation in fMRI signal involved the division of two small numbers, thus errors may propagate nonlinearly. To assess the possibility of false-positive findings, Monte Carlo simulations were performed in which random noise was added to a set of simulated data assuming no differences between normocapnia and hypercapnia. The results showed that the false-positive rate was  $\sim 5.3\%$ , consistent with the  $P$  threshold used ( $P=0.05$ ). Thus, the nonlinear calculation did not seem to cause excessive false-positive rate. The simulations also suggested that the potential errors in the reported percentage changes ( $-20.1\%$ ) were about  $\pm 12.5\%$ .

The T2-relaxation-under-spin-tagging technique determines venous oxygenation based on a T2-preparation sequence. This sequence uses nonselective pulses to avoid the effect of blood flow on the T2 estimation, as discussed in our previous reports (Lu and Ge, 2008; Xu et al, 2009). Blood flow under hypercapnia is faster, thus additional considerations are needed. Assuming a flow velocity of 46 cm/s in the sagittal sinus under hypercapnia, the travel distance under our T2-preparation duration (160 milliseconds) is estimated to be 7.4 cm. This is well within the coverage of the body coil of our MR system.

In summary, our findings suggest that increased CO<sub>2</sub> levels cause the brain to reduce metabolism and spontaneous neural activity, and enter a lower arousal state.

## Disclosure/conflict of interest

The authors declare no conflict of interest.

## References

- Alper KR, John ER, Brodie J, Gunther W, Daruwala R, Prichep LS (2006) Correlation of PET and qEEG in normal subjects. *Psychiatry Res* 146:271–82
- Barzilay Z, Britten AG, Koehler RC, Dean JM, Traystman RJ (1985) Interaction of CO<sub>2</sub> and ammonia on cerebral blood flow and O<sub>2</sub> consumption in dogs. *Am J Physiol* 248:H500–7
- Biswal B, Hudetz AG, Yetkin FZ, Haughton VM, Hyde JS (1997) Hypercapnia reversibly suppresses low-frequency fluctuations in the human motor cortex during rest using echo-planar MRI. *J Cereb Blood Flow Metab* 17:301–8
- Biswal B, Yetkin FZ, Haughton VM, Hyde JS (1995) Functional connectivity in the motor cortex of resting human brain using echo-planar MRI. *Magn Reson Med* 34:537–41
- Buchan RJ, Nagata K, Yokoyama E, Langman P, Yuya H, Hirata Y, Hatazawa J, Kanno I (1997) Regional correlations between the EEG and oxygen metabolism in dementia of Alzheimer's type. *Electroencephalogr Clin Neurophysiol* 103:409–17
- Chiarelli PA, Bulte DP, Piechnik S, Jezzard P (2007) Sources of systematic bias in hypercapnia-calibrated functional MRI estimation of oxygen metabolism. *Neuroimage* 34:35–43
- Cohen ER, Ugurbil K, Kim SG (2002) Effect of basal conditions on the magnitude and dynamics of the blood oxygenation level-dependent fMRI response. *J Cereb Blood Flow Metab* 22:1042–53
- Davis TL, Kwong KK, Weisskoff RM, Rosen BR (1998) Calibrated functional MRI: mapping the dynamics of oxidative metabolism. *Proc Natl Acad Sci USA* 95:1834–9
- de Boorder MJ, Hendrikse J, van der Grond J (2004) Phase-contrast magnetic resonance imaging measurements of cerebral autoregulation with a breath-hold challenge: a feasibility study. *Stroke* 35:1350–4
- Deshpande G, Kerssens C, Sebel PS, Hu X (2010) Altered local coherence in the default mode network due to sevoflurane anesthesia. *Brain Res* 1318:110–21
- Dulla CG, Dobelis P, Pearson T, Frenguelli BG, Staley KJ, Masino SA (2005) Adenosine and ATP link PCO<sub>2</sub> to cortical excitability via pH. *Neuron* 48:1011–23
- Fox PT, Raichle ME (1986) Focal physiological uncoupling of cerebral blood flow and oxidative metabolism during somatosensory stimulation in human subjects. *Proc Natl Acad Sci USA* 83:1140–4
- Fraigne JJ, Dunin-Barkowski WL, Orem JM (2008) Effect of hypercapnia on sleep and breathing in unanesthetized cats. *Sleep* 31:1025–33
- Fukuda T, Hisano S, Toyooka H (2006) Moderate hypercapnia-induced anesthetic effects and endogenous opioids. *Neurosci Lett* 403:20–3
- Gourine AV, Llaudet E, Dale N, Spyer KM (2005) ATP is a mediator of chemosensory transduction in the central nervous system. *Nature* 436:108–11
- Greicius MD, Kiviniemi V, Tervonen O, Vainionpaa V, Alahuhta S, Reiss AL, Menon V (2008) Persistent default-mode network connectivity during light sedation. *Hum Brain Mapp* 29:839–47
- Guyton AC, Hall JE (2005) Respiration. In: *Textbook of Medical Physiology* (Guyton AC, Hall JE, eds), 11th ed. Elsevier: Saunders
- Hong LE, Gu H, Yang Y, Ross TJ, Salmeron BJ, Buchholz B, Thaker GK, Stein EA (2009) Association of nicotine addiction and nicotine's actions with separate cingulate cortex functional circuits. *Arch Gen Psychiatry* 66:431–41
- Horovitz SG, Braun AR, Carr WS, Picchioni D, Balkin TJ, Fukunaga M, Duyn JH (2009) Decoupling of the brain's default mode network during deep sleep. *Proc Natl Acad Sci USA* 106:11376–81
- Horvath I, Sandor NT, Ruttner Z, McLaughlin AC (1994) Role of nitric oxide in regulating cerebrocortical oxygen consumption and blood flow during hypercapnia. *J Cereb Blood Flow Metab* 14:503–9
- Jones M, Berwick J, Hewson-Stoate N, Gias C, Mayhew J (2005) The effect of hypercapnia on the neural and hemodynamic responses to somatosensory stimulation. *Neuroimage* 27:609–23
- Kastrup A, Li TQ, Glover GH, Moseley ME (1999) Cerebral blood flow-related signal changes during breath-holding. *AJNR Am J Neuroradiol* 20:1233–8
- Kety SS, Schmidt CF (1948) The effects of altered arterial tensions of carbon dioxide and oxygen on cerebral blood flow and cerebral oxygen consumption of normal young men. *J Clin Invest* 27:484–92

- Kiloh LG, McComas AJ, Osselton JW (1972) *Clinical Electroencephalography* 3rd ed. Appleton-Century-Crofts: New York
- Kim SG, Ugurbil K (1997) Comparison of blood oxygenation and cerebral blood flow effects in fMRI: estimation of relative oxygen consumption change. *Magn Reson Med* 38:59–65
- Kliefoth AB, Grubb Jr RL, Raichle ME (1979) Depression of cerebral oxygen utilization by hypercapnia in the rhesus monkey. *J Neurochem* 32:661–3
- Kogure K, Busto R, Scheinberg P, Reinmuth O (1975) Dynamics of cerebral metabolism during moderate hypercapnia. *J Neurochem* 24:471–8
- Levy RH, Mattson RH, Meldrum BS (1995) *Antiepileptic Drugs*. 4th ed. New York: Raven Press
- Lu H, Ge Y (2008) Quantitative evaluation of oxygenation in venous vessels using T2-relaxation-under-spin-tagging MRI. *Magn Reson Med* 60:357–63
- Maandag NJ, Coman D, Sangahalli BG, Herman P, Smith AJ, Blumenfeld H, Shulman RG, Hyder F (2007) Energetics of neuronal signaling and fMRI activity. *Proc Natl Acad Sci USA* 104:20546–51
- Mantini D, Perrucci MG, Del Gratta C, Romani GL, Corbetta M (2007) Electrophysiological signatures of resting state networks in the human brain. *Proc Natl Acad Sci USA* 104:13170–5
- Moosmann M, Ritter P, Krastel I, Brink A, Thees S, Blankenburg F, Taskin B, Obrig H, Villringer A (2003) Correlates of alpha rhythm in functional magnetic resonance imaging and near infrared spectroscopy. *Neuroimage* 20:145–58
- Niedermeyer E, da Silva FHL (2005) *Electroencephalography: Basic Principles, Clinical Applications, and Related Fields*. 5th ed. Philadelphia: Lippincott Williams & Wilkins
- Novack P, Shenkin HA, Bortin L, Goluboff B, Soffe AM (1953) The effects of carbon dioxide inhalation upon the cerebral blood flow and cerebral oxygen consumption in vascular disease. *J Clin Invest* 32:696–702
- Rostrup E, Law I, Blinkenberg M, Larsson HB, Born AP, Holm S, Paulson OB (2000) Regional differences in the CBF and BOLD responses to hypercapnia: a combined PET and fMRI study. *Neuroimage* 11:87–97
- Shulman RG, Rothman DL, Hyder F (1999) Stimulated changes in localized cerebral energy consumption under anesthesia. *Proc Natl Acad Sci USA* 96:3245–50
- Sicard KM, Duong TQ (2005) Effects of hypoxia, hyperoxia, and hypercapnia on baseline and stimulus-evoked BOLD, CBF, and CMRO<sub>2</sub> in spontaneously breathing animals. *Neuroimage* 25:850–8
- Xiong J, Parsons LM, Gao JH, Fox PT (1999) Interregional connectivity to primary motor cortex revealed using MRI resting state images. *Hum Brain Mapp* 8:151–6
- Xu F, Ge Y, Lu H (2009) Non-invasive quantification of whole-brain cerebral metabolic rate of oxygen by MRI. *Magn Reson Med* 62:141–8
- Yang SP, Krasney JA (1995) Cerebral blood flow and metabolic responses to sustained hypercapnia in awake sheep. *J Cereb Blood Flow Metab* 15:115–23
- Zappe AC, Uludag K, Logothetis NK (2008a) Direct measurement of oxygen extraction with fMRI using 6% CO<sub>2</sub> inhalation. *Magn Reson Imaging* 26:961–7
- Zappe AC, Uludag K, Oeltermann A, Ugurbil K, Logothetis NK (2008b) The influence of moderate hypercapnia on neural activity in the anesthetized nonhuman primate. *Cereb Cortex* 18:2666–73

Supplementary Information accompanies the paper on the Journal of Cerebral Blood Flow & Metabolism website (<http://www.nature.com/jcbfm>)